Published in final edited form as:
J Tissue Eng Regen Med. 2011 April ; 5(4): 283–291. doi:10.1002/term.313.

Hybrid PGS-PCL Microfibrous Scaffolds with Improved Mechanical and Biological Properties

Shilpa Sant[1,2], **Chang Mo Hwang**[1,2,3], **Sang-Hoon Lee**[3], and **Ali Khademhosseini**[1,2,*]

[1] Center for Biomedical Engineering, Department of Medicine, Brigham and Women's Hospital, Harvard Medical School, 65 Landsdowne Street, Cambridge, MA 02139, USA

[2] Harvard-MIT Division of Health Sciences and Technology, Massachusetts Institute of Technology, Cambridge, MA 02139, USA

[3] Department of Biomedical Engineering, College of Health Science, Korea University, Jeongneung-dong, Seongbuk-gu, Seoul 136-703, Republic of Korea

Abstract

Poly(glycerol sebacate) (PGS) is a biodegradable elastomer that has generated great interest as a scaffold material due to its desirable mechanical properties. However, the use of PGS in tissue engineering is limited by the difficulties to cast micro and nanofibrous structures due to high temperatures and vacuum required for its curing and limited solubility of the cured polymer. In this paper, we developed microfibrous scaffolds made from blends of PGS and poly (ε-caprolactone) (PCL) by using standard electrospinning set up. At a given PGS:PCL ratio, higher voltage resulted in significantly smaller fiber diameters (from ~ 4 μm to 2.8 μm, $p < 0.05$). Further increase in voltage resulted in the fusion of fibers. Similarly, higher PGS concentrations in the polymer blend resulted in significantly increased fiber diameter ($p < 0.01$). We further compared mechanical properties of electrospun PGS:PCL scaffolds with those made from PCL. Scaffolds with higher PGS concentration showed higher elastic modulus (EM), ultimate tensile strength (UTS) and ultimate elongation (UE) ($p < 0.01$) without the need for thermal curing or photocrosslinking. Biological evaluation of these scaffolds showed significantly improved HUVEC attachment and proliferation compared to PCL-only scaffolds ($p < 0.05$). Thus, we have demonstrated that simple blends of PGS prepolymer with PCL can be used to fabricate microfibrous scaffolds with mechanical properties in the range of human aortic valve leaflet.

Keywords

Poly (glycerol sebacate); elastomer; fibers; electrospinning; polycaprolactone; tissue engineering

1. Introduction

Tissue engineering is a promising approach to fulfill the chronic shortage of human donors for tissue and organ transplantations. A key element of this approach is the scaffold, which provides support to the seeded cells as well as desired mechanical properties for tissue regeneration and remodeling (Khademhosseini *et al.* 2009). The ideal scaffold material

*Corresponding author. Phone: 617-768-3495. alik@rics.bwh.harvard.edu.

Author contribution statement: SS and AK designed the study; SS performed the scaffold optimization, characterization and cell culture experiments; CMH performed SEM characterization, mechanical tests and cell culture experiments, SS and CMH analyzed data; SS, CMH, SHL and AK discussed the results; SS wrote the first draft of the paper. All the authors read and commented on the draft.

should be biodegradable, biocompatible and have tunable mechanical properties suitable for each specific application. To fulfill these requirements, research efforts are directed to synthesize new biomaterials with improved chemical, biological and mechanical properties.

Poly(glycerol-sebacate) (PGS) is a biocompatible and biodegradable elastomeric polymer (Wang *et al.* 2002) that has emerged as a promising scaffold material for tissue engineering applications (Fidkowski *et al.* 2005; Sundback *et al.* 2005; Radisic *et al.* 2007; Chen *et al.* 2008; Engelmayr *et al.* 2008; Gao *et al.* 2008; Radisic *et al.* 2008; Hacking and Khademhosseini 2009; Redenti *et al.* 2009). PGS can be easily synthesized from glycerol and sebacic acid, which have been previously approved by FDA (Wang *et al.* 2002). Biocompatibility studies of PGS (Wang *et al.* 2002; Wang *et al.* 2003; Motlagh *et al.* 2006) have shown improved cellular response and hemocompatibilty both in vitro and in vivo. However, despite encouraging results, PGS processability into nano-/microfibers still remains a challenge.

Fibrous scaffolds are considered advantageous for tissue engineering due to their extracellular matrix (ECM) mimicking properties, high surface area to volume ratio and anisotropic mechanical properties (Li *et al.* 2006; Liao *et al.* 2006; Kumbar *et al.* 2008; Soffer *et al.* 2008; Mauck *et al.* 2009). Such fibrous structures are favorable for handling tensile loads while maintaining relatively low bending rigidities (Mauck *et al.* 2009; Sacks *et al.* 2009). Also, the contact guidance provided by these fibers can be used to regulate cell orientation and migration (Ma *et al.* 2005; Hwang *et al.* 2008; Hwang *et al.* 2009; Mauck *et al.* 2009). Thus, the ability to fabricate PGS fibers may be beneficial for tissue engineering applications by simultaneously providing contact guidance and superior mechanical properties. However, it is challenging to cast fibrous PGS scaffolds because PGS prepolymer has to be processed by thermal curing at high temperature and vacuum to convert it into a tough elastomer (Nijst *et al.* 2007; Ifkovits *et al.* 2008; Yi and Lavan 2008). PGS prepolymer itself has low solution viscosity and hence, cannot be electrospun to form stable fibers. Recently, two studies have reported fabrication of PGS fibers by core-shell electrospinning and photocrosslinking, respectively. In one study, Yi and coworkers (Yi and Lavan 2008) obtained PGS fibers by core-shell electrospinning of PGS/poly-L-lactide (PLLA) blends followed by thermal curing of PGS core and dissolution of PLLA shells. In another approach, Ifkovitz et al (Ifkovits *et al.* 2008) blended acrylated PGS with high molecular weight polyethylene oxide followed by photocrosslinking to obtain stable PGS fibers. Recently, this group also blended gelatin with photocrosslinkable PGS to generate fibrous scaffolds with tunable mechanical and degradation properties (Ifkovits *et al.* 2009). Thin (150 μm) scaffolds implanted in vivo were degraded in 2 weeks whereas thicker scaffolds (300 μm) degraded slowly over the period of 4 weeks.

In this work, we fabricated elastomeric microfibrous scaffolds by using blends of non-acrylated PGS prepolymer with FDA approved biodegradable poly(ε-caprolactone) (PCL). PCL is a semicrystalline hydrophobic polymer widely used for electrospinning (Boland *et al.* 2006; Baker *et al.* 2008; Kim 2008; Lee *et al.* 2008; Balguid *et al.* 2009; Del Gaudio *et al.* 2009). However, it shows poor cell behavior due to its hydrophobicity. Other studies have successfully modified PCL with natural polymers such as gelatin and collagen to improve cell attachment, spreading and proliferation (Ma *et al.* 2005; Ghasemi-Mobarakeh *et al.* 2008; Powell and Boyce 2009); however, this approach decreased the mechanical properties of PCL (Ghasemi-Mobarakeh *et al.* 2008). In this work, we blended PGS with PCL. The addition of PCL increased the viscosity of polymer blend making PGS prepolymer suitable for electrospinning. In addition, stable scaffolds were obtained without further processing such as thermal curing or photocrosslinking. Fabricated scaffolds were evaluated for their mechanical and biological properties. PGS:PCL scaffolds showed mechanical properties that were similar to human aortic valve. Interestingly, the addition of

PGS improved cell attachment, spreading and proliferation of Human Umbilical Vein Endothelial Cells (HUVECs) as compared to PCL-only scaffolds. Taken together, we demonstrated that the combination of PGS and PCL can complement their individual properties such as processability, mechanical properties and biological behaviour to improve the scaffold performance for tissue engineering applications.

2. Materials and Methods

2.1 Materials

All the chemicals and solvents including PCL (molecular weight 70,000–90,000), anhydrous chloroform, and absolute ethanol were purchased from Sigma-Aldrich (WI, USA), unless otherwise specified. PGS (molecular weight 12,000) was a kind gift from Dr. Joost Bruggeman, Langer Lab, Department of Chemical Engineering, MIT. All cell culture supplies were purchased from Invitrogen (CA, USA) unless otherwise specified.

2.2. Fabrication of PGS-PCL fibrous scaffolds

PGS:PCL fibers with different compositions were spun by using conventional electrospinning setup. Stable fibers could not be collected using aluminum foil as a collector; hence copper wire wrapped around a glass slide was used as a collector. Fibers were collected on the non-adhesive tape attached on this copper wire frame. To study the effects of PGS:PCL ratio as well as applied voltage on the fiber morphology and diameter, PGS and PCL were dissolved at different weight ratios (5:1, 3:1, 2:1 and 0:1, respectively) in anhydrous chloroform: ethanol mixture (9:1) and electrospun at 12.5, 15, 17.5 and 20 kV. The total polymer concentration was kept constant at 33% w/v. Pure PCL scaffolds were electrospun using 16 % w/v polymer solution because it was difficult to electrospin highly viscous 33% w/v PCL solution. Other parameters such as the distance between the needle and the collector (18 cm), flow rate (2 mL/h) and needle diameter (21G) were kept constant during fiber fabrication. Scaffolds were spun for 30 min for each condition and dried overnight in a desiccator to remove any remaining solvent prior to further use.

2.3. Scanning electron microscopy (SEM) of scaffolds

To characterize the fiber morphology of the electrospun PGS-PCL meshes, field emission scanning electron microscope (FE SEM) Ultra 55 (Carl Zeiss, Inc. NY, USA) was used. For SEM observation, electrospun scaffolds were dried under vacuum and coated with ion coater with palladium-platinum target materials. For ion coating, ion current was controlled to 40 mA for 80 sec prior to SEM morphological examination. The images were captured at 5kV. Fiber diameter measurements were performed on at least three different SEM images with 20 fibers per image using ImageJ software (NIH, http://rsbweb.nih.gov/ij/).

2.4. Contact angle measurements of scaffolds

The hydrophilicity of the PCL-only and PGS:PCL scaffolds was determined by contact angle measurements. The contact angle of electrospun scaffolds was measured by a video contact angle system (VCA Optima, AST Inc.). An average value of three measurements was reported with standard deviation.

2.5. Mechanical properties of electrospun scaffolds

For mechanical characterization of the electrospun scaffolds, uniaxial elongation test was performed with an Instron 5542 mechanical tester (Norwood, MA, USA). Electrospun meshes were dried for atleast 48 h under vacuum to ensure complete removal of solvents, cut to rectangular shape with $5 \times 15 mm^2$. Specimens were inserted into the grips with 10 mm gap as initial dimension of test region. During uniaxial test, initial strain rate was set as

25% of original test regional length and the crosshead speed was set constant at 2.5 mm/min. Five specimens from different batches were tested for each condition. Elastic moduli (EM) were calculated from the 0–5% strain region in the stress-strain curve. Ultimate strength (UTS) and ultimate elongation (UE) were measured form the highest peak of stress-strain curve. Three data from each condition were selected from the test results. Values were reported as mean ± standard deviation (SD).

2.6. Human Umbilical Vein Endothelial Cell (HUVEC) attachment and proliferation

2.6.1. HUVEC culture—GFP transfected HUVECs were a kind gift from the laboratory of Dr. Judah Folkman, Children's Hospital, Boston. HUVECs were cultured in EBM-2 (Endothelial Cell Basal Medium-2, Lonza, MD, USA) supplemented with the provided growth factor kit. The cell cultures were maintained at 37 °C and 5% CO2 and media was changed twice a week.

2.6.2. Cell seeding—Scaffolds were sterilized by soaking in 70% ethanol for at least 12 h prior to the cell seeding and washed thoroughly with Dulbecco's phosphate buffered saline (DPBS). Cells were seeded on each scaffold {0.5 cm (l) × 0.5 cm (w) × 200 μm (t)} at final concentration of 1×10^5 cells/scaffold in 24-well tissue culture plates (TCP) and allowed to attach for 6 h. The scaffolds with the attached cells were then transferred to another dish prior to long term incubation.

2.6.3. Cell attachment, spreading and proliferation—HUVECs were seeded on the scaffolds as described above. After 6 h, the scaffolds were washed three times with DPBS to remove loosely attached/unattached cells. Cells were then fixed with 4% formaldehyde, and washed with DPBS. Scaffolds were dehydrated with a series of alcohols, and dried in a critical point dryer (Auto Samdri 815 Series A, Tousimis, MD, USA). Cell attachment and cell spreading were observed using FE-SEM, Ultra 55 after palladium-platinum as described above. Also, confocal laser scanning microscope (Olymplus FV300) was used to study the cell morphology after 1 week culture period.

Quantitative evaluation of cell attachment (after 8 h) and proliferation was performed using Alamar Blue (AB) assay as per manufacturer's instructions (Invitrogen, CA, USA). This assay enables time course analysis of cell proliferation by measuring the ability of viable cells to reduce resazurin dye (blue) to resorufin (pink). Reduction of AB is proportional to the number of living cells. Briefly, cells were seeded on scaffolds (n=3) as described above. After 8 h, scaffolds with adherent cells were transferred to a new dish containing fresh medium. Cells seeded on TCPs served as control. AB dissolved in RPMI1640 (0.5 mL, 10% v/v) was added into each well and incubated for 3 h at 37°C. Reduced AB (100 μL) was then transferred to 96-well plate in triplicate and absorbance was measured at 570 and 600 nm. The percentage of AB reduced was calculated as per manufacturer's protocol. Change in cell proliferation was also calculated by normalizing the % AB reduced with respect to that on day 0 for each scaffold.

2.7. Statistical analysis

All data were expressed as mean ± SD. Statistical comparisons between two groups were done using student's paired t-test while multiple comparisons were done using one-way/two-way ANOVA followed by post-hoc Tukey test (OriginPro8 SRO, v8.07). Differences at p-value less than 0.05 were considered to be statistically significant unless otherwise noted. All error bars were presented as standard deviations.

3. Results and discussion

PGS is a tough biodegradable elastomer originally developed by Wang et al (Wang *et al.* 2002) for soft tissue engineering applications. Three-dimensional PGS scaffolds have already shown great promise in tissue engineering (Fidkowski *et al.* 2005; Sundback *et al.* 2005; Radisic *et al.* 2007; Chen *et al.* 2008; Engelmayr *et al.* 2008; Gao *et al.* 2008; Radisic *et al.* 2008; Redenti *et al.* 2009). This approach consisted of seeding cells of interest either on films or on porous PGS scaffolds. However, high temperatures (> 80° C) and vacuum conditions required for PGS processing makes fabrication of complex micro/nanostructured scaffolds difficult (Nijst *et al.* 2007). Electrospinning offers a versatile tool for fabrication of micro-/nanofibrous scaffolds from natural and synthetic polymers. It has been suggested that nano-/microscale surface topographies significantly influence cell behaviors such as adhesion, orientation, migration and proliferation by mimicking the topography of ECM (Khademhosseini *et al.* 2006; Hwang *et al.* 2009). In this work, we hypothesized that preparation of fibrous scaffolds of PGS elastomer can improve the scaffold performance by providing essential contact guidance to the seeded cells within mechanically dynamic environment. Recently, Ifkovits et al (Ifkovits *et al.* 2008; Ifkovits *et al.* 2009) and Yi et al (Yi and Lavan 2008) have shown the possibility of fabricating fibrous scaffolds using acrylated PGS and coaxial electrospinning using PGS/PLLA blends, respectively. In both of these methods, post-processing such as photocrosslinking or thermal curing of as-spun scaffolds was required. Here, we report fabrication of PGS-based fibers with enhanced mechanical and biological properties by using blends of non-acrylated PGS prepolymer with PCL. This approach can be performed on a typical electrospinning setup without any need for post-processing steps.

3.1. Morphology and wettability of PGS-PCL fibrous scaffolds

Various parameters that affect electrospinning include polymer properties, solution properties, applied electrical potential, distance between needle and collector (working distance) and type of collector (Liao *et al.* 2006; Xie *et al.* 2008). Various collectors have been used in the past including aluminum foil, rotating drum/mandrel, and parallel plate (Liao *et al.* 2006; Kumbar *et al.* 2008; Xie *et al.* 2008). Here, we used a collector in which copper wire was wrapped around a glass slide and fibers were collected on a non-adhesive side of adhesive tape attached onto this collector. Effect of different ratios of PGS to PCL and voltage on fiber formation was studied while keeping the total polymer concentration (33 % w/v), working distance (18 cm) and flow rate (0.5 mL/h) constant. As PGS prepolymer is less viscous, PGS:PCL polymer blends at higher PGS ratio (5:1 and 3:1) resulted in less viscous solutions. Hence, fibers could be obtained only at 12.5 and 15 kV for these solutions. Higher PCL content in 2:1 PGS:PCL polymer blends resulted in sufficient viscosity to obtain fibers at all voltage conditions. In fact, one of the main reasons for difficulty in electrospinning PGS prepolymer is its low viscosity even at high polymer concentration as reported by Yi et al (Yi and Lavan 2008).

We observed that the degree of fiber alignment, morphology and diameter was also affected by PGS:PCL ratio as well as the applied voltage. At the same applied voltage, fiber diameters increased significantly from 2.76 ± 0.03 μm for pure PCL to 6.77 ± 0.26 μm for 5:1 PGS:PCL scaffolds ($n = 20$ fibers for 3 different images, $p < 0.01$) as shown in Fig. 1B. This was due to decreased solution viscosity at higher PGS ratio. Generally, minimum amount of polymer chain entanglement and viscosity is necessary for electrospinning fibers. At lower viscosity, higher amount of solvent molecules and fewer polymer chain entanglements result in dominant surface tension effects resulting in bead or spindle formation (Kumbar *et al.* 2008). Bead formation was also observed for higher PGS:PCL ratio at 12.5 kV when anhydrous chloroform alone was used as a solvent (data not shown).

However, addition of 10% ethanol reduced the surface tension leading to smooth fiber formation without beads.

Similarly, at the same PGS:PCL ratio (2:1), increase in the voltage from 12.5 kV to 17.5 kV reduced fiber diameters significantly from 3.99 ± 0.22 μm to 2.89 ± 0.2 μm, respectively ($p < 0.05$). However, further increase in the voltage resulted in two fold increase in the fiber diameter from 3.99 ± 0.22 μm (at 12.5 kV) to 8.25 ± 0.31 μm (at 20 kV, $p < 0.05$) (Fig. 1C). These findings are in accordance with previous reports (Kumbar *et al.* 2008). Initially, increasing the voltage may have increased the amount of charges in the jet and higher stretching resulting in reduced fiber diameter. Further increase in the voltage may result in instability of the jet and fusion of fibers leading to thicker fibers.

Contact angle measurements were done to study the hydrophilicity/wettability of the PGS:PCL scaffolds. PCL-only scaffolds showed high contact angle of 130 ± 3°. Interestingly, for all PGS-containing scaffolds, water drop dispensed on the scaffolds was not stable and completely wetted the scaffolds within few seconds. These studies demonstrated that addition of PGS improved the hydrophilicity of the scaffolds.

3.2. Mechanical properties

Mechanical testing was carried out using fibers prepared with different PGS:PCL ratio. Diameter of these fibers varied from 2.7 to 8.7 μm from PCL, 2:1, 3:1 and 5:1 PGS:PCL ratio, respectively. Fig. 2A shows the linear region of stress-strain curve for all the scaffolds in the first 15% of the strain region. Although PCL, 2:1 and 3:1 PGS:PCL scaffolds showed comparable elastic modulus (EM) of about 10 MPa, 5:1 scaffolds showed 3–4 folds increase in EM (Fig. 2B). Similar trend was observed for ultimate tensile strength (UTS) as shown in Fig. 2C, where 5:1 scaffolds showed approximately 1.5 times increased UTS. Interestingly, ultimate elongation (UE) of pure PCL scaffold was found to be 626.66 ±15.2 % whereas reported values for PCL electrospun scaffolds were in the range of 200–300% (Chen *et al.* 2008;Mauck *et al.* 2009). All the PGS:PCL scaffolds showed UE in the range of 400–600 % (Fig. 2D).

The EM, UTS and UE are representative of stiffness, strength and elasticity respectively. Thus, 2:1 and 3:1 PGS:PCL scaffolds showed lower stiffness (EM) and lower elasticity (elongation) whereas 5:1 PGS:PCL scaffolds showed higher strength (UTS), higher stiffness and similar elasticity compared to pure PCL scaffolds. As shown in Fig. 1, variation in PGS:PCL ratio resulted in changes in the fiber morphology (Fig. 1A) as well as fiber diameter (Fig. 1B). These factors play an important role in determining the mechanical properties of electrospun scaffolds (Mauck *et al.* 2009). For instance, 2:1 PGS:PCL scaffolds showed smaller diameter and welded fiber morphology; while 3:1 PGS:PCL scaffolds showed increased diameter with single fiber morphology. On the other hand, 5:1 PGS:PCL scaffolds resulted more tightly packed fiber morphology than 3:1 ratio even though fiber diameter did not change significantly. Thus, welded fiber morphology of both 2:1 and 5:1 PGS:PCL scaffolds may have resulted in higher UTS and elongation than 3:1 scaffolds. Further addition of PGS at 5:1 PGS:PCL ratio resulted in simultaneous increase in EM, UTS and elongation for 5:1 PGS:PCL. The exact reason for this is not known; however, the amount of PGS, the degree of fiber alignment and fiber morphology (individual fibers against welded fibers) could be the factors responsible for such mechanical properties of the scaffolds (Mauck *et al.* 2009;Powell and Boyce 2009).

It is interesting to note that EM of photocured acrylated PGS films also varied from 0.15–30 MPa whereas UE achieved was only up to 200% (Ifkovits *et al.* 2008). On the other hand, thermally cured PGS films have shown UTS less than 1 MPa and UE of about 200–400 % (Wang *et al.* 2002; Chen *et al.* 2008). Thus, microfibrous PGS:PCL scaffolds could be

fabricated with similar elasticity, but higher ultimate strength without any thermal or photocrosslinking. It is also worthwhile to note that PCL blends with natural materials such as gelatin resulted in reduced mechanical properties (Ghasemi-Mobarakeh *et al.* 2008) whereas addition of PGS resulted in comparable or even superior mechanical properties. Furthermore, the enhancement of tensile strength is generally accompanied by reduced elasticity (Rafat *et al.* 2008). However, simultaneous enhancement of all mechanical properties was achieved for 5:1 PGS:PCL scaffolds without thermal or UV crosslinking, thus resulting in a tougher material. Such high EM and UTS combined with high UE may be useful for artificial heart valve leaflet tissue engineering. These values correlated well with those reported by Balguid et al for native human aortic valve leaflets (Balguid *et al.* 2007). The authors have found that human aortic leaflets have EM of 15.6 ± 6.4 MPa and UTS of 2.6 ± 1.2 MPa. Thus, PGS:PCL scaffolds may be promising for engineered heart valve leaflets and the studies are underway to test this possibility.

3.3. Cell attachment, spreading and proliferation

GFP-labeled HUVECs were seeded on pure PCL scaffolds as well as PGS:PCL scaffolds prepared with different ratios. Fig. 3A shows the SEM images of cells seeded on PCL and PGS:PCL 5:1 scaffolds after 6 h post-seeding. It was found that cells remained rounded on hydrophobic PCL scaffolds whereas they could easily spread on PGS:PCL scaffolds. SEM images clearly showed that cells did not only spread on PGS:PCL scaffolds but also completely surrounded these scaffolds within a short period of 6 h. Quantitative analysis of cell attachment by AB assay clearly showed significantly reduced number of cells on PCL as compared to TCP and PGS:PCL scaffolds ($p < 0.05$ Fig. 3B). However, addition of PGS to PCL resulted in improved cell attachment almost equivalent to TCP, which was considered as a positive control. Confocal laser scanning microscope images taken after 1 week in culture also revealed that fibers provided appropriate surface for guided cell attachment (Fig. 3C).

Similarly, cell proliferation was significantly lower on PCL scaffolds compared to TCP ($p < 0.05$) as shown in Fig. 4A. Amount of PGS in the scaffolds did not result in any significant difference in cell proliferation on PGS containing scaffolds ($p > 0.05$) as all PGS scaffolds showed comparable cell metabolic activity. Also, all PGS:PCL scaffolds showed proliferation comparable to TCP until day 2 after which cells proliferated much faster on TCP than scaffolds. This was in accordance with previously published data (Ma *et al.* 2005). However, when cell proliferation was normalized to day 0 reading of the respective scaffolds (reported as folds change in proliferation with respect to day 0), high content PGS scaffolds (3:1 and 5:1) showed change in proliferation equivalent to TCP whereas pure PCL showed significantly slower change in proliferation ($p < 0.05$). Improved cell data on PGS:PCL scaffolds clearly showed that PGS promoted cell attachment and proliferation on these scaffolds.

Although electrospun PCL mimics many aspects of natural ECM structure, its poor hydrophilicity leads to lower cell adhesion, proliferation and differentiation. Contact angle measurements revealed contact angle of 130° f o r PCL-only scaffolds indicating their hydrophobic nature. Generally, hydrophilic/hydrophobic properties of the scaffolds influence cell adhesion and proliferation (Ghasemi-Mobarakeh *et al.* 2008). In fact, various studies have successfully improved cellular behaviour of PCL by blending it with natural polymers like gelatin or collagen (He *et al.* 2005; Ma *et al.* 2005; Ghasemi-Mobarakeh *et al.* 2008; Del Gaudio *et al.* 2009; Powell and Boyce 2009). In our study, contact angle measurements revealed improved wettability of PGS containing scaffolds compared to PCL-only scaffolds. Interestingly, 3:1 and 5:1 scaffolds were wetted completely immediately after addition of water drop. Thus, improved cell adhesion and proliferation on PGS containing scaffolds may be attributed to the higher hydrophilicity of these scaffolds compared to pure

PCL alone. Also, insignificant differences in cell adhesion and proliferation of PGS containing scaffolds may be due to their similar hydrophilicity.

Conclusion

In this study, we successfully fabricated fibrous scaffolds by blending PGS elastomeric polymers with PCL. PGS and PCL blends could be useful to overcome a number of limitations associated with each material. For instance, the addition of PCL (18–33 % of total polymer blend) increased the solution viscosity to enable fiber formation by electrospinning. On the other hand, presence of PGS significantly improved cell attachment, spreading and proliferation as compared to pure PCL scaffolds. Although PGS prepolymer was used, mechanical properties of the PGS:PCL scaffolds were comparable to thermally or photocrosslinked polymer sheets even though no crosslinking method was used. At the same time, PGS-PCL scaffolds did not result decreased mechanical properties as compared to PCL-only scaffolds. Overall, the mechanical properties of the scaffolds were in the range of native human aortic valve. Interestingly, simultaneous increase in ultimate tensile strength was achieved without compromising ultimate elongation. In other words, tough scaffolds with high elasticity could be fabricated motivating further studies towards their potential application tissue engineering.

Acknowledgments

This paper was supported by the National Institutes of Health (EB007249; DE019024; HL092836) and the US Army Core of Engineers. SS acknowledges the postdoctoral fellowship received by Fonds de Recherche sur la Nature et les Technologies (FQRNT), Quebec, Canada. The authors thank Dr. Jason Nichol for his useful comments and help with PGS.

References

Baker BM, Gee AO, Metter RB, et al. The potential to improve cell infiltration in composite fiber-aligned electrospun scaffolds by the selective removal of sacrificial fibers. Biomaterials. 2008; 29(15):2348–2358. [PubMed: 18313138]

Balguid A, Mol A, van Marion MH, et al. Tailoring Fiber Diameter in Electrospun Poly(epsilon-Caprolactone) Scaffolds for Optimal Cellular Infiltration in Cardiovascular Tissue Engineering. Tissue Eng Part A. 2009; 15(2):437–444. [PubMed: 18694294]

Balguid A, Rubbens MP, Mol A, et al. The role of collagen cross-links in biomechanical behavior of human aortic heart valve leaflets - Relevance for tissue engineering. Tissue Eng. 2007; 13(7):1501–1511. [PubMed: 17518750]

Boland, ED.; Pawlowski, KJ.; Barnes, CP., et al. Electrospinning of bioresorbable polymers for tissue engineering scaffolds. In: Reneker, DH.; Fong, H., editors. Polymeric Nanofibers. Vol. 918. 2006. p. 188-204.

Chen QZ, Bismarck A, Hansen U, et al. Characterisation of a soft elastomer poly(glycerol sebacate) designed to match the mechanical properties of myocardial tissue. Biomaterials. 2008; 29(1):47–57. [PubMed: 17915309]

Del Gaudio C, Bianco A, Folin M, et al. Structural characterization and cell response evaluation of electrospun PCL membranes: Micrometric versus submicrometric fibers. J Biomed Mater Res Part A. 2009; 89A(4):1028–1039.

Engelmayr GC, Cheng MY, Bettinger CJ, et al. Accordion-like honeycombs for tissue engineering of cardiac anisotropy. Nat Mater. 2008; 7(12):1003–1010. [PubMed: 18978786]

Fidkowski C, Kaazempur-Mofrad MR, Borenstein J, et al. Endothelialized microvasculature based on a biodegradable elastomer. Tissue Eng. 2005; 11(1–2):302–309. [PubMed: 15738683]

Gao J, Crapo P, Nerern R, et al. Co-expression of elastin and collagen leads to highly compliant engineered blood vessels. J Biomed Mater Res Part A. 2008; 85A(4):1120–1128.

Ghasemi-Mobarakeh L, Prabhakaran MP, Morshed M, et al. Electrospun poly(epsilon-caprolactone)/gelatin nanofibrous scaffolds for nerve tissue engineering. Biomaterials. 2008; 29(34):4532–4539. [PubMed: 18757094]

Hacking SA, Khademhosseini A. Applications of Microscale Technologies for Regenerative Dentistry. Journal of Dental Research. 2009; 88(5):409–421. [PubMed: 19493883]

He W, Ma Z, Yong T, et al. Fabrication of collagen-coated biodegradable polymer nanofiber mesh and its potential for endothelial cells growth. Biomaterials. 2005; 26(36):7606–7615. [PubMed: 16000219]

Hwang CM, Khademhosseini A, Park Y, et al. Microfluidic chip-based fabrication of PLGA microfiber scaffolds for tissue engineering. Langmuir. 2008; 24(13):6845–6851. [PubMed: 18512874]

Hwang CM, Park Y, Park JY, et al. Controlled cellular orientation on PLGA microfibers with defined diameters. Biomed Microdevices. 2009; 11(4):739–746. [PubMed: 19242806]

Ifkovits JL, Devlin JJ, Eng G, et al. Biodegradable Fibrous Scaffolds with Tunable Properties Formed from Photo-Cross-Linkable Poly(glycerol sebacate). ACS Appl Mater Interfaces. 2009; 1(9):1878–1886. [PubMed: 20160937]

Ifkovits JL, Padera RF, Burdick JA. Biodegradable and radically polymerized elastomers with enhanced processing capabilities. Biomed Mater. 2008; 3(3):1–8.

Khademhosseini A, Langer R, Borenstein J, et al. Microscale technologies for tissue engineering and biology. Proceedings of the National Academy of Sciences of the United States of America. 2006; 103(8):2480–2487. [PubMed: 16477028]

Khademhosseini A, Vacanti JP, Langer R. Progress in tissue engineering. Scientific American. 2009; 300(5):64–71. [PubMed: 19438051]

Kim GH. Electrospun PCL nanofibers with anisotropic mechanical properties as a biomedical scaffold. Biomed Mater. 2008; 3(2):8.

Kumbar SG, James R, Nukavarapu SP, et al. Electrospun nanofiber scaffolds: engineering soft tissues. Biomed Mater. 2008; 3(3):1–15.

Lee SJ, Oh SH, Liu J, et al. The use of thermal treatments to enhance the mechanical properties of electrospun poly (epsilon-caprolactone) scaffolds. Biomaterials. 2008; 29(10):1422–1430. [PubMed: 18096219]

Li CM, Vepari C, Jin HJ, et al. Electrospun silk-BMP-2 scaffolds for bone tissue engineering. Biomaterials. 2006; 27(16):3115–3124. [PubMed: 16458961]

Liao S, Li B, Ma Z, et al. Biomimetic electrospun nanofibers for tissue regeneration. Biomed Mater. 2006; 1(3):R45–53. [PubMed: 18458387]

Ma Z, He W, Yong T, et al. Grafting of gelatin on electrospun poly(caprolactone) nanofibers to improve endothelial cell spreading and proliferation and to control cell Orientation. Tissue Eng. 2005; 11(7–8):1149–1158. [PubMed: 16144451]

Ma Z, Kotaki M, Inai R, et al. Potential of nanofiber matrix as tissue-engineering scaffolds. Tissue Eng. 2005; 11(1–2):101–109. [PubMed: 15738665]

Mauck RL, Baker BM, Nerurkar NL, et al. Engineering on the Straight and Narrow: The Mechanics of Nanofibrous Assemblies for Fiber-Reinforced Tissue Regeneration. Tissue Eng Part B Rev. 2009; 15(2):171–193. [PubMed: 19207040]

Motlagh D, Yang J, Lui KY, et al. Hemocompatibility evaluation of poly(glycerol-sebacate) in vitro for vascular tissue engineering. Biomaterials. 2006; 27(24):4315–4324. [PubMed: 16675010]

Nijst CLE, Bruggeman JP, Karp JM, et al. Synthesis and characterization of photocurable elastomers from poly(glycerol-co-sebacate). Biomacromolecules. 2007; 8(10):3067–3073. [PubMed: 17725319]

Powell HM, Boyce ST. Engineered Human Skin Fabricated Using Electrospun Collagen-PCL Blends: Morphogenesis and Mechanical Properties. Tissue Eng Part A. 2009; 15(8):2177–2187. [PubMed: 19231973]

Radisic M, Park H, Gerecht S, et al. Biomimetic approach to cardiac tissue engineering. Philos Trans R Soc B-Biol Sci. 2007; 362(1484):1357–1368.

Radisic M, Park H, Martens TP, et al. Pre-treatment of synthetic elastomeric scaffolds by cardiac fibroblasts improves engineered heart tissue. J Biomed Mater Res Part A. 2008; 86A(3):713–724.

Rafat M, Li F, Fagerholm P, et al. PEG-stabilized carbodiimide crosslinked collagen-chitosan hydrogels for corneal tissue engineering. Biomaterials. 2008; 29(29):3960–3972. [PubMed: 18639928]

Redenti S, Neeley WL, Rompani S, et al. Engineering retinal progenitor cell and scrollable poly(glycerol-sebacate) composites for expansion and subretinal transplantation. Biomaterials. 2009; 30(20):3405–3414. [PubMed: 19361860]

Sacks MS, Schoen FJ, Mayer JE. Bioengineering Challenges for Heart Valve Tissue Engineering. Annual Review of Biomedical Engineering. 2009; 11(1):289–313.

Soffer L, Wang XY, Mang XH, et al. Silk-based electrospun tubular scaffolds for tissue-engineered vascular grafts. J Biomater Sci-Polym Ed. 2008; 19(5):653–664. [PubMed: 18419943]

Sundback CA, Shyu JY, Wang YD, et al. Biocompatibility analysis of poly(glycerol sebacate) as a nerve guide material. Biomaterials. 2005; 26(27):5454–5464. [PubMed: 15860202]

Wang YD, Ameer GA, Sheppard BJ, et al. A tough biodegradable elastomer. Nat Biotechnol. 2002; 20(6):602–606. [PubMed: 12042865]

Wang YD, Kim YM, Langer R. In vivo degradation characteristics of poly(glycerol sebacate). J Biomed Mater Res Part A. 2003; 66A(1):192–197.

Xie JW, Li XR, Xia YN. Putting Electrospun Nanofibers to Work for Biomedical Research. Macromol Rapid Commun. 2008; 29(22):1775–1792. [PubMed: 20011452]

Yi F, Lavan DA. Poly(glycerol sebacate) nanofiber scaffolds by core/shell electrospinning. Macromol Biosci. 2008; 8(9):803–806. [PubMed: 18504802]

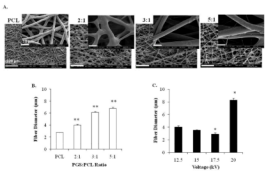

Figure 1.
Effect of PGS:PCL ratio and voltage on fiber morphology and diameter. Scanning electron microscopic images of fibrous scaffolds; A) Effect of PGS:PCL ratio on the fiber morphology at 12.5kV; Scale bar is 100 μm, inset scale bar is 10 μm. B) Effect of PGS:PCL ratio on fiber diameter. Fiber diameter increased significantly with increased PGS ratio (**$p < 0.01$) compared to PCL-only scaffolds. At least 20 fibers were measured in 3 different image fields for each condition. C) Effect of voltage on fiber diameter at 2:1 PGS:PCL ratio. Fiber diameter decreased significantly with increasing voltage up to an optimum voltage (17.5kV) after which fibers fused to form large fibers (*$p<0.05$ compared to 12.5 kV). Statistical analysis was carried out using One-way ANOVA followed by post-hoc Tukey test.

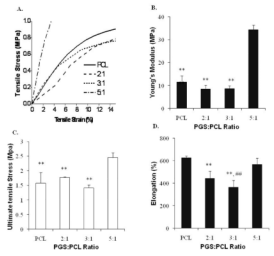

Figure 2.

Mechanical properties of PGS:PCL fibrous scaffolds; A) Linear region of stress-strain curve for PGS:PCL scaffolds; B) Young's modulus, as calculated from 0–5% linear region of stress-strain curve, C) Ultimate tensile strength, and D) Elongation at break. Mechanical properties varied as a function of PGS:PCL ratio and fiber morphology. Scaffolds prepared with 5:1 PGS:PCL ratio showed highest Young's modulus, tensile strength and elongation compared to other scaffolds. Population means were significantly different from each other (n=3, One-way ANOVA, **: $p < 0.01$ compared to 5:1 PGS:PCL scaffolds; ##: $p < 0.01$ compared to PCL scaffolds).

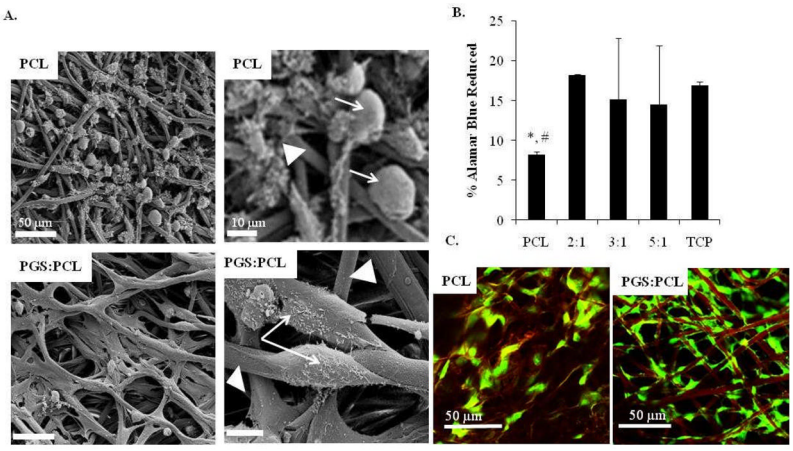

Figure 3.

Evaluation of cell attachment and cell morphology on PGS:PCL fibrous scaffolds; A) Scanning electron microscopic images of HUVEC attachment and spreading on fibrous scaffolds 6 h post-seeding; (scale bar: left panel 50 μm and right panel 10 μm). Cells and fibers are marked with white arrow and white triangle, respectively. Cells remained rounded on PCL fibers whereas they spread on PGS:PCL fibers after 6 h as shown by the arrows in magnified images in the right panel. B) Quantitative analysis of HUVEC attachment by AB assay 8 h post-seeding; Cells were incubated with AB reagent for 3 h and ability of attached cells to reduce AB was calculated. Scaffolds containing PGS did not show significant difference compared to cells grown on TCP as control ($p > 0.05$) whereas pure PCL scaffolds showed significantly reduced cell attachment ($p < 0.05$, *: compared to TCP and #: 2:1 PGS:PCL scaffolds). Statistical analysis was carried out using One-way ANOVA followed by post-hoc Tukey test. C) Confocal laser scanning images of cells (green) seeded on PCL-only and PGS:PCL scaffolds after 1 week in culture.

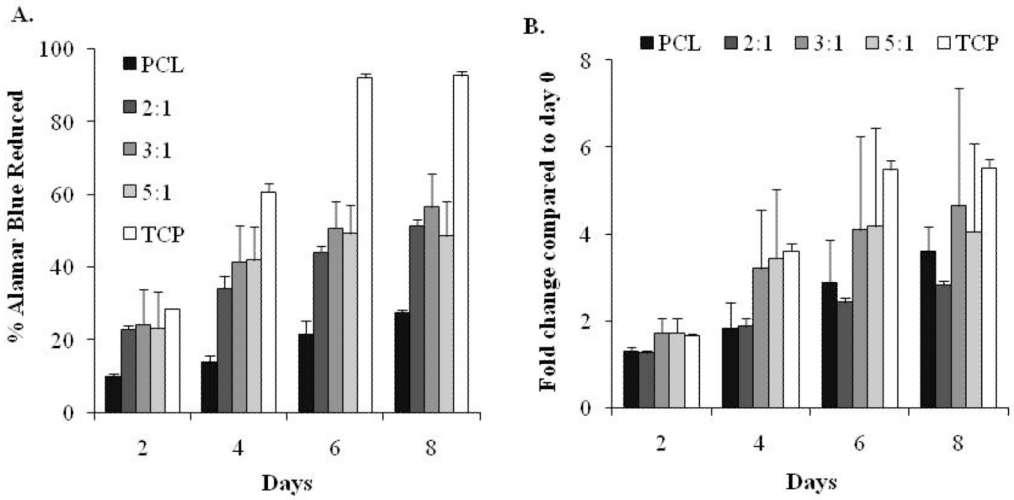

Figure 4.

Evaluation of cell proliferation on PGS:PCL fibrous scaffolds; A) HUVEC proliferation on PGS:PCL scaffolds by AB assay; HUVEC cells were seeded onto scaffolds and tissue culture wells for 8 days and cell proliferation was analyzed by measuring their ability to reduce the resazurin (blue) to resorufin (pink). Percentage of AB reduction was directly proportional to live HUVECs. Cell proliferation was significantly slower on PCL scaffolds as compared to TCP and PGS:PCL scaffolds ($p < 0.05$) whereas PGS:PCL scaffolds did not show significant difference amongst themselves ($p > 0.05$). For the same scaffolds, proliferation increased significantly from day 0 to day 6 ($p < 0.05$) after which it reached a plateau. B) Fold change in proliferation for each scaffold (n=3) as compared to Day 0. Scaffolds prepared with higher PGS:PCL ratio resulted in comparable proliferation change as in TCP; however PCL scaffolds and 2:1 PGS:PCL scaffolds showed significantly slower proliferation as compared to TCP ($p < 0.05$); Statistical analysis was carried out using One-way ANOVA followed by post-hoc Tukey test.